Magnetic properties of the superconducting polymers $(SN)_x$ and $(SNBr_{0.4})_x$

R. H. Dee,* J. F. Carolan, and B. G. Turrell
Department of Physics, University of British Columbia, Vancouver, British Columbia, Canada V6T 1W5

R. L. Greene
IBM Research Laboratory, San Jose, California 95193
(Received 16 January 1980)

The magnetizations of the superconducting sulfur nitrogen polymer $(SN)_x$ and its brominated modification, $(SNBr_{0.4})_x$, have been studied as a function of magnetic field and temperature. There is anisotropy in the magnetization observed in both materials. However, $(SNBr_{0.4})_x$ behaves more like a bulk superconductor than $(SN)_x$ does, indicating stronger interfiber coupling in the former.

I. INTRODUCTION

Polymeric sulfur nitride $(SN)_x$ has attracted considerable attention because it exhibits anisotropic properties both in its normal and superconducting states.[1] Recently it has been shown[2] that $(SN)_x$ can be reacted with halogens to form new polymers whose electronic properties are significantly altered.[3,4] To date the derivative most studied is the bromine modification $(SNBr_{0.4})_x$ denoted hereafter as SNBr. The object of these investigations has been the elucidation of the structure of this material and of the role of the bromine atoms in the conduction process.

One dominant feature of these materials is their fibrous nature, the fiber diameter being about 100 Å in $(SN)_x$ and about half that size in SNBr. In the normal state the fibers have the effect of masking the bulk properties. Thus, the anisotropy in the electrical conductivity observed in dc measurements is much larger than that determined from optical measurements.[5] In the superconducting state the situation is quite complicated. $(SN)_x$ and SNBr behave neither like bulk superconductors nor systems of uncoupled fibers; rather they appear to be filamentary superconductors with some coupling between fibers. Although there has been considerable speculation on the properties of multiconnected superconductors ever since the "sponge" model proposed by Mendelssohn,[6] these systems are still not completely understood. In this paper measurements of the low-field magnetizations of the two materials as a function of applied field and temperature are presented and an estimate of the interfiber coupling is attempted. Preliminary results of these measurements have been reported[7,8] and the work presented here extends those measurements by calibrating the magnetization and using samples of different purity and dimensions.

II. EXPERIMENTAL

The $(SN)_x$ crystals used in this study were synthesized using established techniques.[9] One sample was taken from a batch synthesized at the University of British Columbia (UBC) denoted as $(SN)_x$(UBC) on which uncalibrated measurements have been reported by Dee *et al.*[7] Another sample was taken from a batch synthesized at IBM San Jose denoted as $(SN)_x$(IBM). From this batch a few crystals were taken and exposed to bromine vapor at room temperature for 24 h. Excess bromine was then removed by pumping on the samples for 1 h. The resulting samples of SNBr were blue black and in the form of small chunks. The dimensions of the samples used are listed in Table I.

The measurements of the dc magnetization were made in a manner similar to earlier work.[7] As indicated in Fig. 1 the sample under study was placed in one half of a pair of coils which were wound astatically and which formed part of a superconducting flux transformer coupled to a superconducting quantum interference device (SQUID). The sample was cooled to low temperature by mounting it and the coils on a copper cold finger attached to the mixing chamber of a dilution refrigerator. Magnetic fields were applied using a superconducting solenoid wound on the 1 K heat shield of the refrigerator. Stability was achieved by using the magnet in the persistent mode. The whole assembly was surrounded by a superconducting lead shield to reduce the ambient magnetic field and external electromagnetic noise.

TABLE I. Summary of results.

		$(SN)_x$(UBC)[a]	$(SN)_x$(IBM)	$(SNBr_{0.4})_x$[b]
Sample dimensions (mm^3)		$0.6\times0.45\times0.45$	$0.92\times0.85\times0.5$	$1.2\times0.8\times0.45$
Residual resistance ratio	RRR	3	25	8[c]
Fraction of full diamagnetic signal on warming $H=0.025$ Oe, $T=59$ mK	$H_\perp$	0.25 ± 0.04	0.63 ± 0.04	1.00 ± 0.05
	$H_\parallel$	0.05 ± 0.01	0.15 ± 0.01	0.57 ± 0.04
Magnetic critical temperature (mK)	T_c	230 ± 10	280 ± 10	308 ± 10
Applied field corresponding to peak in magnetization ($T=59$ mK)	$H_{p\perp}$	0.70 ± 0.06	0.70 ± 0.06	2.25 ± 0.1
	$H_{p\parallel}$	0.18 ± 0.02	0.19 ± 0.02	0.75 ± 0.07
Effective penetration depth (mm) for $H=0.025$ Oe, $T=59$ mK	$\lambda_e(H_\perp)$		~0.05	$0.001-0.01$
	$\lambda_e(H_\parallel)$		~0.1	0.05

[a]This is the uncalibrated sample reported in Ref. 7.
[b]The $(SNBr_{0.4})_x$ sample was from the same batch as $(SN)_x$(IBM) and is the sample reported in Ref. 8.
[c]This value is estimated from measurements on similar crystals.

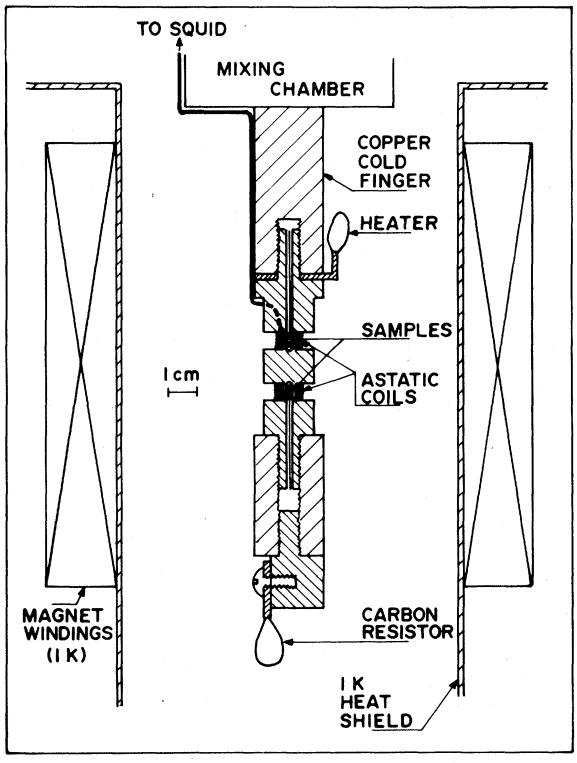

FIG. 1. A diagram of the apparatus showing the relative positions of the pickup coils and samples.

Application of a magnetic field H_a to the sample produced a change in the flux observed by the SQUID of $\Delta\phi_s$. For the case of an ellipsoidal sample this change in the flux is related to the change in the sample magnetization ΔM_s by the relation

$$-4\pi\Delta M_s = H_a/(1-n_s) = A_s\Delta\phi_s \ . \quad (1)$$

Here n_s is the demagnetizing factor defined such that it would be $\frac{1}{3}$ for a sphere. The factor A_s includes geometrical and coupling factors between the sample and the pickup coils and could not be accurately calculated for our sample and coil configuration. Also our samples were not ellipsoidal and could not be so shaped by machining or cutting due to their small size and mechanical properties. In order to make quantitative measurements of the sample magnetization, we compared the magnetization of our samples with a reference sample made of the superconducting alloy $In_{0.90}$-$Pb_{0.10}$ and cut to the same dimensions as the $(SN)_x$ or SNBr sample.

Assuming that demagnetizing and coupling effects were the same in both the reference samples and their matching $(SN)_x$ or SNBr samples, their magnetizations can be compared by simply comparing measured flux changes, i.e.,

$$\Delta M_s/\Delta M_r = \Delta\phi_s/\Delta\phi_r \ , \quad (2)$$

where $\Delta\phi_r$ and ΔM_r are the flux and magnetization changes, respectively, for the reference sample. In

making these measurements the appropriate InPb reference sample was placed in one half of the astatic coil assembly, allowing direct comparison of the flux changes between it and the $(SN)_x$ or SNBr sample located in the other coil of the pair. It was assumed that the InPb alloy exhibited a full Meissner effect for the small fields applied.

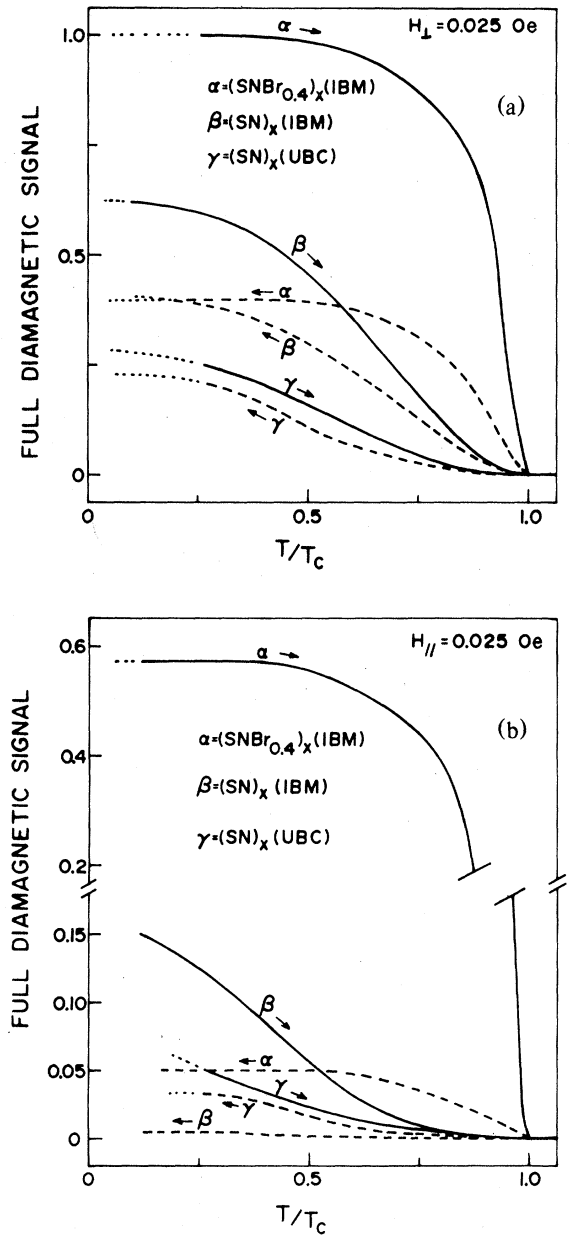

FIG. 2. Magnetization of two samples of $(SN)_x$ and one sample of $(SNBr_{0.4})_x$ as a function of reduced temperature for a field of 0.025 Oe applied (a) perpendicular to the fiber axis and (b) parallel to the fiber axis. The critical temperatures T_c are given in Table I.

The lower critical fields also can be estimated in the experiment. Although our samples are not ellipsoidal, we make the approximation that demagnetization effects can be represented by a demagnetization factor which we estimate to be $n_s = 0.2-0.4$ from the sample dimensions.[10] We can then relate the lower critical field H_{c1} for a type-II superconductor to the field H_p at which the magnetization reaches its peak value by the expression

$$H_{c1} = H_p/(1-n_s) \quad . \tag{3}$$

The measurements were made with the crystals mounted with the fiber axis oriented either parallel or perpendicular to the measuring coil axis. The error in alignment was estimated to be $< 3°$. After initially cooling the samples in zero applied field, magnetization versus temperature curves were obtained by warming in a constant applied field. Magnetization curves as a function of applied field could then be derived from such sets of data. The zero of the applied field (± 0.0005 Oe) was obtained by adjusting the solenoid current to produce no detectable change in magnetization in the reference sample at its superconducting transition at 4.5 K.

III. EXPERIMENTAL RESULTS

Figure 2 shows the low-field magnetization measurements. Data for fields applied perpendicular and parallel to the fiber axis of the crystals are shown in Figs. 2(a) and 2(b), respectively. The magnetic field in each case was applied after the sample had been cooled to a low temperature ($\sim 30-50$ mK) in zero field (~ 0.0005 Oe). The samples were then warmed to 0.35 K and cooled again in the applied field to determine how much magnetic flux was ex-

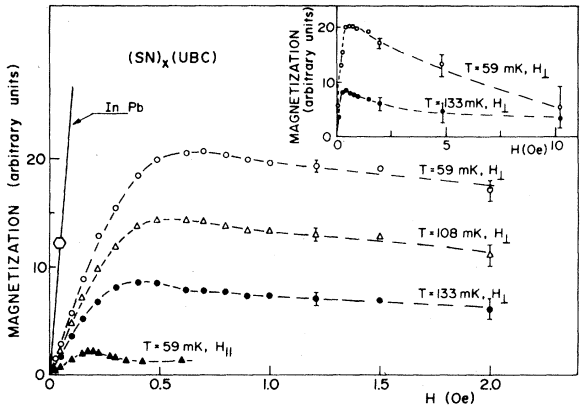

FIG. 3. Magnetization of $(SN)_x$(UBC) as a function of magnetic field at various temperatures. The low-field part of the magnetization curve for the calibrating sample InPb is also shown.

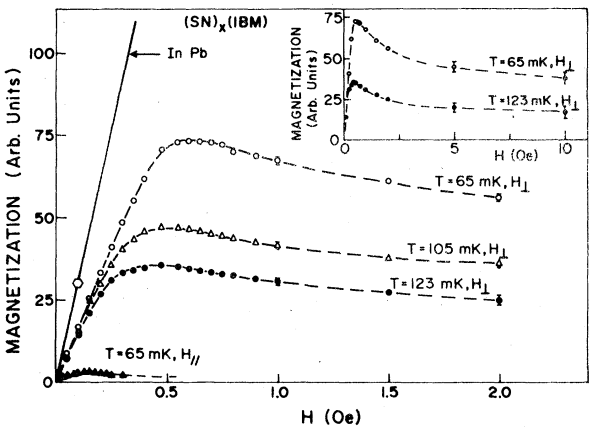

FIG. 4. Magnetization of $(SN)_x$(IBM) as a function of magnetic field at various temperatures plus the low-field portion of the magnetization of the calibration sample of InPb.

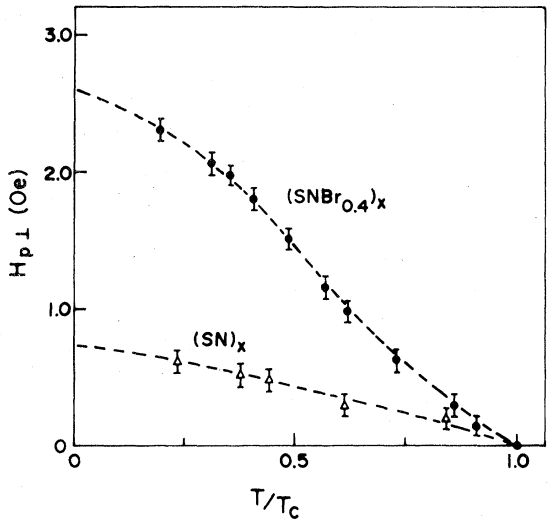

FIG. 6. Field at which the magnetization reaches its peak $H_{p\perp}$, for fields applied perpendicular to the fiber axis vs reduced temperature for the IBM samples.

pelled and how much was trapped. The magnitude of the magnetization of SNBr in a given field is much larger than $(SN)_x$ and in the perpendicular orientation it exhibits the full diamagnetic response expected for a superconductor. Also the transition in SNBr occurs over a much narrower temperature range, and the cooling data show that there is a higher degree of flux trapping in SNBr.

The anisotropy in the materials is better illustrated when we extract magnetization curves as a function of field. These are shown in Figs. 3, 4, and 5 for $(SN)_x$(UBC), $(SN)_x$(IBM), and SNBr, respectively. For $(SN)_x$ the magnetization rises nonlinearly to a peak before decreasing slightly at higher fields. The peak in the magnetization curves for both $(SN)_x$ samples occurs at the same field value and has the same anisotropy (see Table I). After bromination these peaks shift to higher fields but the anisotropy remains. The dependence of the peak fields on temperature is shown in Fig. 6.

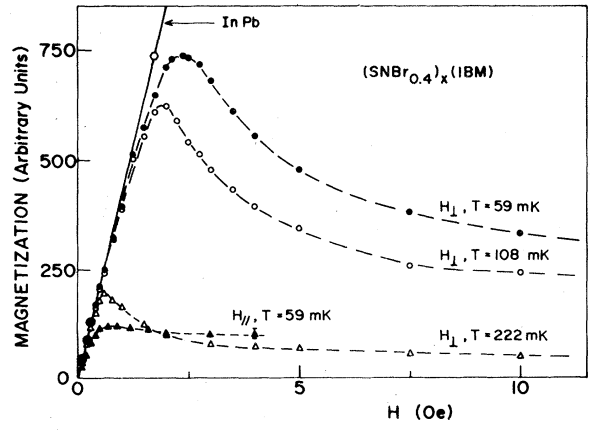

FIG. 5. Magnetization of $(SNBr_{0.4})_x$ as a function of magnetic field at various temperatures plus the low-field portion of the magnetization of the calibration sample of InPb.

IV. DISCUSSION

The data shown in Fig. 2 show that, for the applied field applied parallel to the fiber axis, none of the samples behave like a bulk superconductor which gives a full diamagnetic response. This is perhaps not too surprising given the fibrous nature of the materials. In fact, we can calculate the London penetration depth λ_L for $(SN)_x$ using the optical data[5] and we obtain the result

$$\lambda_L = c/\omega_p \approx 2700 \text{ Å} ,$$

where c is the velocity of light and ω_p is the plasma frequency. A value of similar magnitude is obtained for SNBr. We can also estimate an effective London penetration depth λ_e from our magnetization data using Schoenberg's expression[11]

$$M \approx \frac{H}{4\pi(n_s-1)}\left(1-\frac{\alpha\lambda_e}{l}\right) , \tag{4}$$

where α is a geometrical factor of order unity and l is a characteristic diameter or thickness of the sample measured in a direction perpendicular to the applied field. Note that Eq. (4) is valid only when $\lambda_e < l$. This relation predicts that M is proportional to λ_e/l; i.e., there is an effect due to size. A size effect actu-

ally is observed; if we compare the two $(SN)_x$ samples the UBC sample was smaller than the IBM sample and did exhibit a smaller diamagnetic response. The values of λ_e for the various cases calculated using Eq. (4) are listed in Table I. For H applied perpendicular to the fiber axis the dominant penetration is assumed to be along the crystal b-axis direction along the fibers. For H applied parallel to the fiber axis, the penetration is perpendicular to the fibers and the dimension of the sample in the ab plane is the relevant parameter in estimating l. The value of n_s used is the effective demagnetizing factor estimated from the sample dimensions and the value of M is taken to be the low-temperature limit of the magnetization. Note that there is anisotropy in the calculated values of λ_e and that λ_e approaches the value of λ_L only for the case of field applied perpendicular to the fibers of SNBr.

That the polymers do not act like bulk superconductors is also supported by the temperature dependence of the magnetization. For the bulk superconductor the London penetration depth varies with temperature as[11]

$$\lambda_L(T)=\lambda_L(0)[1-(T/T_c)^4]^{-1/2} \quad . \tag{5}$$

In fact it is impossible to fit our data using Eqs. (4) and (5) even for the case $H_\perp$ in SNBr. Our conclusion is that the superconducting properties of these materials are greatly influenced by their fibrous morphology.

Having demonstrated that the fibrous nature of the materials is important, it is interesting to consider a model for the sample consisting of a bundle of completely uncoupled fibers. For the case of $(SN)_x$ with fiber diameter $d\approx 100$ Å, this would imply $\lambda_L >> d$. In this limit the magnetization would be reduced by a factor of $\frac{1}{32}(d/\lambda_L)^2\approx 4\times 10^{-4}$ from the full diamagnetic value. Obviously the observed magnetizations are greater so that the fibers cannot be completely uncoupled. A similar argument can be applied to the case of SNBr in which the fibers are even finer. In fact, in this case, the observed magnetization is of greater magnitude than for $(SN)_x$.

From our analysis we conclude that the magnitude of the observed magnetization is between the value one expected for simply connected bulk material of millimeter dimensions and the value estimated for uncoupled fibers of diameter 100 Å. To discuss this problem of a multiconnected anisotropic fibrous system we adopt the anisotropic effective-mass approximation used for layered systems.[12] We analyze the SNBr because the upper critical field is well established allowing the coherence length perpendicular to the fibers to be estimated to be $\xi_\perp\approx 100$ Å. Combining this with the thermodynamic critical field of $H_c\approx 20$ Oe obtained from the critical temperature,[1,4] we find

$$\lambda_\perp\approx\sqrt{2}\phi_0/(4\pi H_c\xi_\perp)=1.4\times 10^{-3}\text{ mm}$$

and

$$H_{c1\parallel}\approx\frac{H_c\ln(\lambda_\perp/\xi_\perp)}{\sqrt{2}\lambda_\perp\xi_\perp}=0.15\text{ Oe} \quad .$$

Here ϕ_0 is one flux quantum and we have assumed approximate validity of the Ginzburg-Landau theory away from the transition region.[13] Similarly, for fields perpendicular to the fibers we find $\lambda_\parallel\approx 3.5\times 10^{-4}$ mm and $H_{c1\perp}\approx 3.9$ Oe. The value of $\lambda_\parallel$ should be the dominant component of the measured $\lambda_e(H_\perp)$ of Table I and it is within the range measured for $\lambda_e(H_\perp)$. We can compare the calculated $H_{c1\perp}$ to experiment by noting from Table I the value of $H_{p\perp}=2.25$ Oe. Taking into account the effective demagnetizing factor $n_s=0.2$–0.4 we find from Eq. (3)

$$H_{c1\perp}=3\text{–}4\text{ Oe} \quad .$$

While this is in agreement with the value calculated above, we should note that there is significant nonlinearity in the magnetization curve (Fig. 5) for $H<H_{p1}$. This may simply be due to large scale cracks and inhomogeneities in the sample, or it may reflect the breakdown of this theory for such fibrous materials.[14]

For the field parallel to the fibers of SNBr these questions become more important. The magnetization (Fig. 5) is even more distorted from the ideal type-II behavior. If we use Eq. (3) with the observed SNBr peak value $H_p=0.75$ Oe, we find $H_{c1\parallel}\approx 0.9$–$1.3$ Oe. This value is much larger than the calculated value of 0.15 Oe. Also, the experimental value for the penetration depth (0.05 mm) is much larger than the calculated value 1.4×10^{-3} mm. This discrepancy could be due to a breakdown in the theory as has been observed in TaS_2,[15] or it could simply be explained by H_{c1} being much less than H_p for fields parallel to the fibers. This would be the case if at $H_{c1}\approx 0.15$ Oe there were penetration of the field into the material, but the fibrous structure behaved like a hard type-II material inhibiting the motion of the flux. Such behavior is predicted in the hard superconductors modeled by Bean.[16] In fact the significant flux trapping observed in our data (Figs. 2–4) lends credence to this interpretation.

It is difficult to make a similar analysis of the $(SN)_x$ data due to the difficulties in determining $\xi_\perp$ from H_{c2}.[4] However, because these difficulties exist and because there is increased nonlinearity observed in the magnetization data for $H<H_p$ for both orientations of the magnetic field, we conclude that there is less coupling between fibers in the $(SN)_x$ system. This conclusion is further supported by the magnitude of the diamagnetism being less in $(SN)_x$ than in SNBr as mentioned above.

ACKNOWLEDGMENTS

We thank G. B. Street of IBM for generously supplying the samples and D. H. Dollard for help in the early phase of the experiments. Work at UBC was supported by the National Sciences and Engineering Research Council of Canada. Work at IBM was supported by the Office of Naval Research.

---

*Present address: S.H.E. Corp., San Diego, Calif.

[1]R. L. Greene and G. B. Street, in *Chemistry and Physics of One Dimensional Metals,* edited by H. J. Keller (Plenum, New York, 1977), p. 69.

[2]W. D. Gill, W. Bludeau, R. H. Geiss, P. M. Grant, R. L. Greene, J. J. Mayerle, and G. B. Street, Phys. Rev. Lett. 38, 1305 (1977).

[3]C. K. Chaing, M. J. Cohen, D. L. Peebles, A. J. Heeger, M. Akktar, J. K. Leppinger, A. G. McDiarmid, J. Milliken, and M. J. Moran, Solid State Commun. 23, 607 (1977).

[4]J. F. Kwak, R. L. Greene, and W. W. Fuller, Phys. Rev. B 20, 2658 (1979).

[5]P. M. Grant, R. L. Greene, and G. B. Street, Phys. Rev. Lett. 35, 1743 (1975).

[6]K. Mendelssohn, Proc. R. Soc. London, Ser. A 152, 34 (1935).

[7]R. H. Dee, D. H. Dollard, B. G. Turrell, and J. F. Carolan, Solid State Commun. 24, 469 (1977).

[8]R. H. Dee, J. F. Carolan, B. G. Turrell, R. L. Greene, and G. B. Street, J. Phys. (Paris) Colloq. 39, C6-444 (1978).

[9]G. B. Street, H. Arnal, W. D. Gill, P. M. Grant, and R. L. Greene, Mater. Res. Bull. 10, 877 (1975).

[10]G. W. Crabtree, Phys. Rev. B 16, 1117 (1977); D. E. Prober, M. R. Beasley, and R. E. Schwall, Phys. Rev. B 15, 5245 (1977).

[11]D. Shoenberg, *Superconductivity* (Cambridge, London, 1952), p. 233.

[12]P. deTrey, S. Gygax, and J. P. Jan, J. Low Temp. Phys. 11, 421 (1973).

[13]M. Tinkham, *Introduction to Superconductivity* (McGraw-Hill, New York, 1975), p. 156.

[14]C. M. Bastuscheck, R. A. Buhrman, H. Temkin, and J. C. Scott, Bull. Am. Phys. Soc. 23, 305 (1978).

[15]S. Gygax, J. Low Temp. Phys. 36, 109 (1979).

[16]C. P. Bean, Phys. Rev. Lett. 8, 250 (1962).